

Article

A Two-Dimensional Liquid Sloshing Analysis in a Partially Filled Complicated-Shape Tank by the Schwarz–Christoffel Transformation

Jing Lü *, Xiaolong Zhu  and Yang Yu 

Department of Dynamics and Control, Beihang University, Beijing 100191, China; zhuxiaolong009@163.com (X.Z.); yu.yang@buaa.edu.cn (Y.Y.)

* Correspondence: lvjing@buaa.edu.cn

Abstract: The nonlinear sloshing of an incompressible fluid with irrotational flow in a complicated-shape tank due to horizontal excitation is studied with a semi-analytical method proposed in this study. In this method, the velocity potential function of a liquid in a complicated-shape tank is estimated by using an approximate analytical transformation function from a complicated-shape region to a rectangular region. This function is obtained through Schwarz–Christoffel mapping and polynomial fitting. Nonlinear dynamic equations for the fluid–structure coupled system are developed based on the Hamilton–Ostrogradskiy principle. Nonlinear kinematic equations for the fluid–structure coupled system are derived based on the relationship between the liquid velocity and the free-surface equation. The Galerkin method is used to convert partial differential equations into ordinary differential equations. When tank movement is given, nonlinear models for the coupled system can be reduced to simple ones for liquid sloshing. Natural frequencies for the coupled system and liquid sloshing are analyzed, and the semi-analytical results agree with the numerical ones calculated with the software DampSlosh. Hydrodynamic forces and moments are also analyzed, and the semi-analytical results agree well with the numerical ones calculated with the Flow3D v10.1.1.

Keywords: Schwarz–Christoffel transformation; liquid sloshing; complicated-shape tank; natural frequency; hydrodynamic force; hydrodynamic moment



Citation: Lü, J.; Zhu, X.; Yu, Y. A Two-Dimensional Liquid Sloshing Analysis in a Partially Filled Complicated-Shape Tank by the Schwarz–Christoffel Transformation. *Acoustics* **2024**, *6*, 346–361. <https://doi.org/10.3390/acoustics6020018>

Academic Editors: Theodore E. Matikas and Jian Kang

Received: 7 March 2024

Revised: 25 March 2024

Accepted: 3 April 2024

Published: 19 April 2024



Copyright: © 2024 by the authors. Licensee MDPI, Basel, Switzerland. This article is an open access article distributed under the terms and conditions of the Creative Commons Attribution (CC BY) license (<https://creativecommons.org/licenses/by/4.0/>).

1. Introduction

Sloshing is the motion of a liquid in a partially filled container with an unrestrained free surface due to external excitation. Understanding this complicated dynamic behavior is of practical significance, especially when the liquid contributes a non-negligible portion to the total mass, because liquid sloshing is observed in a wide range of engineering applications, such as heavy-duty road tankers, oceangoing vessels, oil tankers, rockets, and aerospace transportation vehicles [1–5]. The primary challenge in sloshing analysis lies in accurately estimating the natural frequencies, hydrodynamic forces, and moments of liquid sloshing. If the excitation frequency is close to natural frequencies, especially the lowest ones, resonance may occur and result in catastrophic consequences. The hydrodynamic forces and moments of sloshing applied to a container may also lead to uncontrollability and structural damage. Furthermore, the containers used in engineering applications are of various shapes, and each individual container shape requires a dedicated applied mathematical and physical study.

Numerous researchers have studied the problem of liquid sloshing, and their research approaches are generally classified as analytical, numerical, and experimental. For analytical approaches, variational formation based on Hamilton’s principle is regarded as the most powerful tool for developing fluid field equations, and the velocity potential function is a key factor in the analytical process. If the fluid motion is irrotational and

incompressible, the velocity potential function should satisfy Laplace's equation. Rectangular coordinates are used to solve Laplace's equation and the boundary condition on the wetted tank surface for rectangular tanks [6–9]. Similarly, cylindrical, bipolar, toroidal, and spherical coordinates are used to solve velocity potential functions for upright cylindrical, horizontal cylindrical, annular cylindrical, and spherical tanks, respectively [10–15]. However, velocity potential functions can be obtained directly by solving Laplace's equation and the boundary condition for a limited number of tank shapes only. Conformal mapping can be used to estimate velocity potential functions for other tank shapes because the velocity potential function of liquid sloshing is harmonic. Nevertheless, conformal mapping is mainly applied to only a few tank shapes, such as half-full horizontal elliptical, horizontal circular, horizontal cylindrical, and spherical, to determine the velocity function of fluid [16–21]. The nonconformal transformation technique and the variational modal approach have been developed for circular conical and prolate spheroidal tanks; one scheme employs a projective approach, and the other is adopted for spectral problems [22–24]. To the knowledge of the authors, the applications of conformal mapping and nonconformal transformation have not been extended to more complicated tank shapes because coordinate transformation from a complicated shape to a simple one is difficult. Numerical and experimental approaches are used to analyze the dynamics of liquid sloshing in tanks with highly complicated shapes [25–28]. However, long-term simulations using numerical approaches yield unrealistic flows and cannot describe steady-state motions. Meanwhile, experimentation is expensive. Therefore, analytical or semi-analytical approaches should be further developed to describe fluid sloshing in tanks with complicated shapes.

With regard to fluid–structure coupled dynamics, a common approach is to model liquid sloshing by using computational fluid dynamics, i.e., using numerical methods such as the ALE method and SPH method, when dealing with a sloshing fluid in a container with an arbitrary shape [29–31]. However, these methods do not always produce reliable results, especially when the sloshing motion is complex [32]. The traditional approach models a sloshing liquid by using an equivalent mechanical model, such as an equivalent pendulum model or an equivalent mass–spring model, which is linear or nonlinear with cubic stiffness; however, nonlinear sloshing is more complicated than these equivalent models, so this method does not consider nonlinear interactions between fluid and structure dynamics and among various slosh modes [33]. Another approach is to model the entire fluid–structure coupled system by adopting the variational principle, in which the liquid is assumed to be inviscid, incompressible, and irrotational. This approach considers nonlinear interactions between liquid and structure dynamics and among various slosh modes but has only been applied to fluid–structure coupled systems with rectangular, cylindrical, and spherical containers [34–36]. The main objective of extending these approaches to other fluid–structure coupled systems with complicated-shape tanks is to describe the fluid field by using an analytic function, that is, to determine the velocity potential function in tanks with complicated shapes.

In this study, a theoretical analysis of nonlinear liquid sloshing and fluid–structure coupled dynamics is performed for tanks with complicated shapes. If the movement of a rigid tank is given, a fluid–structure coupled dynamic model can be reduced to a model that describes only the nonlinear dynamics of liquid sloshing. Therefore, a fluid–structure coupled dynamic model is derived in this study, and natural frequencies, hydrodynamic forces, and moments are analyzed. The main contribution of this study is twofold. First, a semi-analytical method is proposed to estimate the velocity potential function in tanks with complicated shapes. The approximate analytical transformation function from a complicated-shape region to a rectangular region is obtained by Schwarz–Christoffel mapping and polynomial fitting. Second, a nonlinear fluid–structure coupled system model is developed based on the Hamilton–Ostrogradskiy principle and the relationship between the liquid velocity and the free-surface equation. The semi-analytical results of natural frequencies, hydrodynamic forces, and moments are validated by a numerical approach.

The rest of this paper is organized as follows. Section 2 introduces a semi-analytical method for estimating the velocity potential function and wave height function of a liquid in a tank with a complicated shape. Section 3 shows the derivation of the nonlinear fluid–structure coupled system model and an analysis of the natural frequencies of the coupled system, the natural frequencies of the sloshing liquid, and the hydrodynamic forces and moments. Section 4 presents the application of the method to a Cassini-section-shaped tank with different liquid depths. The two walls of the tank are vertical, and the bottom is a semicircle. The semi-analytical results are validated through numerical simulations. Section 5 provides a summary of the investigation.

2. Materials and Methods

A semi-analytical method is proposed to calculate the velocity potential function of a liquid in a tank with a complicated shape. The key point is determining the analytical conformal mapping function from a complicated-shape region to a rectangular region. First, point mapping is performed by using the Schwarz–Christoffel transformation twice; that is, an upper half-plane is mapped to a complicated-shape region and a rectangular region. Second, the polynomial fitting method is adopted to obtain the final approximate analytical mapping function. The velocity potential function of the liquid is harmonic. Thus, by using the approximate analytical mapping function, the velocity potential function of a liquid in a rectangular tank can be mapped as that of a liquid in a complicated-shape tank.

2.1. Analytical Mapping Function

In complex analyses, the Schwarz–Christoffel transformation is a conformal transformation of the upper half-plane to the interior of a simple polygon. The upper half-plane can be mapped to complicated-shape and rectangular regions via Schwarz–Christoffel transformation.

The equation that represents the transformation by which the upper half-plane is mapped to the complicated-shape polygon region is

$$z = f_z(h) = A_z \int_0^h (p - p_1)^{\frac{\theta_1}{\pi}} (p - p_2)^{\frac{\theta_2}{\pi}} \cdots (p - p_{n-1})^{\frac{\theta_{n-1}}{\pi}} dp + B_z, \quad (1)$$

where $z = x + yi$; the x -axis is the real axis, and the y -axis is the imaginary axis on the z -plane; $\theta_1, \theta_2, \dots, \theta_n$ are the internal angles of the polygon; $f_z(h)$ is a complex function; A_z and B_z are constants; and p_1, p_2, \dots, p_{n-1} are the coordinates of points P_1, P_2, \dots, P_{n-1} on the real axis of the h -plane, which are the preimages of angular points z_1, z_2, \dots, z_{n-1} of the polygon on the z -plane. $(-\infty, 0)$ and $(+\infty, 0)$ on the real axis of the h -plane are the preimages of z_n , as shown in Figure 1.

Similarly, the equation that represents the transformation by which the upper half-plane is mapped to the rectangular region is

$$w = f_w(h) = A_w \int_0^h (q - q_1)^{\frac{1}{2}} (q - q_2)^{\frac{1}{2}} (q - q_3)^{\frac{1}{2}} dq + B_w, \quad (2)$$

where $w = u + vi$; the u -axis is the real axis, and the v -axis is the imaginary axis on the w -plane; $f_w(h)$ is a complex function; A_w and B_w are constants; and $q_1, q_2,$ and q_3 are the coordinates of points $Q_1, Q_2,$ and Q_3 on the real axis of the h -plane corresponding to angular points $w_1, w_2,$ and w_3 of the rectangle on the w -plane, respectively. $(-\infty, 0)$ and $(+\infty, 0)$ on the real axis of the h -plane are the preimages of w_4 , as shown in Figure 1.

In sloshing problems, z_k and z_{k+1} correspond to the two end points of the hydrostatic surface in a complicated-shape tank, and w_1 and w_2 correspond to the two end points of the hydrostatic surface in a rectangular tank (Figure 1). Therefore, on the h -plane, points Q_1 and Q_2 should coincide with points P_k and P_{k+1} , respectively. As a result, $z = f_z[f_w^{-1}(w)]$ and $w = f_w[f_z^{-1}(z)]$, which means that the complicated-shape region is mapped to a rectangular region. The mapping of the upper half-plane to a simple triangular domain cannot be evaluated with exact formulas but can be addressed through a numerical approximation.

For highly complicated polygons, the evaluations of Schwarz–Christoffel integrals f_z and f_w in (1) and (2) are almost invariably beyond the scope of exact formulas and should be considered through numerical approaches. Several numerical algorithms based on Newton’s method and Gauss–Jacobi quadrature for solving the Schwarz–Christoffel integrals f_z and f_w are presented in [37]. Then, discrete mapping of any point $z(x, y)$ within the complicated-shape domain onto point $w(u, v)$ within the rectangular domain can be realized. After one-to-one mapping is performed between the interior points of a complicated shape and those of a rectangle, the polynomial fitting method is adopted to generate the approximate analytical expression as follows:

$$\begin{aligned}
 u &= f_u(x, y) = \sum_{n=0}^{\infty} \sum_{j=0}^n \alpha_{nj} x^{n-j} y^j, \\
 v &= f_v(x, y) = \sum_{n=0}^{\infty} \sum_{j=0}^n \beta_{nj} x^{n-j} y^j.
 \end{aligned}
 \tag{3}$$

where $f_u(x, y)$ and $f_v(x, y)$ are real functions.

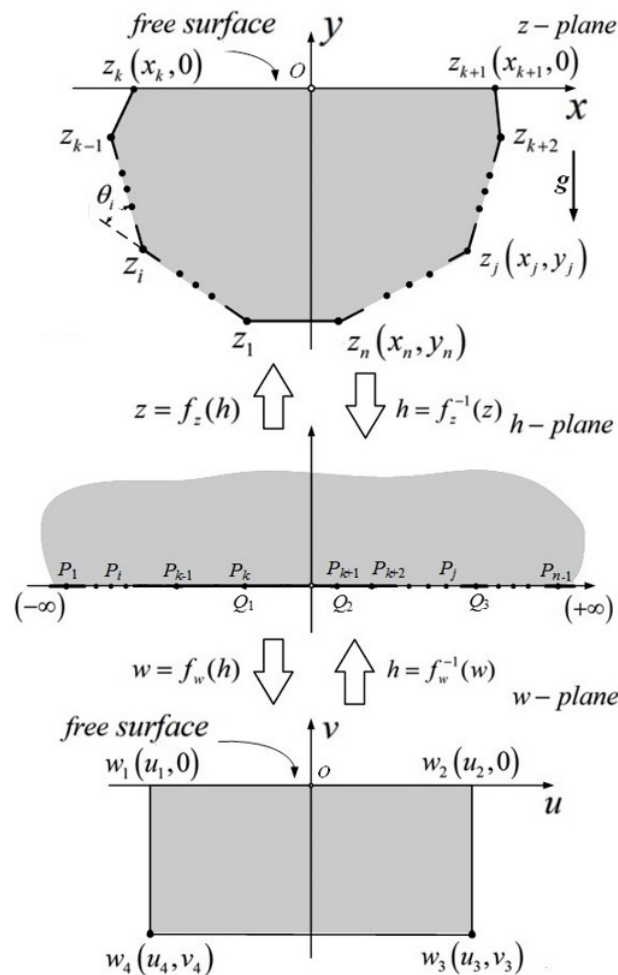


Figure 1. The upper half-plane is mapped to the interior of a polygon and a rectangle.

The most important application of the Schwarz–Christoffel transformation is the construction of a one-to-one mapping function carrying the upper half-plane to the interior of a given polygon. Once curved boundaries are contained in the complicated shape, circumscribed polygons are substituted for the curves.

2.2. Velocity Potential and Wave Height Functions

If a flow is assumed to be irrotational, then the velocity of a liquid in a stationary tank can be expressed as $v = \nabla\phi$, where ϕ is the velocity potential function. Simultaneously, if a flow is incompressible, then ϕ is harmonic, i.e., $\nabla^2\phi = 0$. The normal derivative of ϕ is zero, i.e., $\partial\phi/\partial n = 0$, where n is the normal axis perpendicular to the boundary. A harmonic function ϕ that satisfies the boundary condition $\partial\phi/\partial n = 0$ for a complicated-shape tank can be obtained based on the one for a simple-shape tank by using conformal mapping. The liquid velocity potential function in a complicated-shape tank can be calculated by substituting approximate analytical mapping functions $f_u(x, y)$ and $f_v(x, y)$ into the existing liquid velocity potential function in a rectangular tank as follows:

$$\begin{aligned}\phi &= \sum_{n=1}^{\infty} u_n(t)\psi_n(x, y), \\ \psi_n(x, y) &= \frac{\cosh[k_n(f_v(x, y) + a)]}{k_n \sinh k_n a} \cos k_n \left(f_u(x, y) + \frac{b}{2} \right),\end{aligned}\quad (4)$$

where $u_n(t)$ is a time-dependent coefficient; $k_n = \frac{n\pi}{b}$; and a and b are the width and height of the rectangle, respectively.

The wave function of a liquid in a complicated-shape tank can be determined by

$$\begin{aligned}\zeta &= \sum_{n=1}^{\infty} v_n(t)\zeta_n(x), \\ \zeta_n(x) &= \left. \frac{\partial\psi_n(x, y)}{\partial y} \right|_{y=y_0},\end{aligned}\quad (5)$$

where ζ is the wave height function; $v_n(t)$ is a time-dependent coefficient; and y_0 is the coordinate of the hydrostatic surface in the complicated-shape tank.

3. Results

Using the velocity potential function of the liquid partially filling the complicated-shape tank that is derived by the semi-analytical method, the nonlinear dynamics caused by horizontal excitation can be studied.

Potential flow theory is applied, and the main assumptions are as follows: the fluid is incompressible and the flow within the tank is irrotational, the fluid is inviscid and the flow is non-turbulent, the liquid surface does not overturn or break, and the amplitude of the sloshing waves is small compared to the dimensions of the tank. The nonlinear fluid–structure coupled dynamic equations are derived based on the Hamilton–Ostrogradskiy principle. The nonlinear kinetic equations are deduced based on the relationship between the liquid velocity and the disturbed liquid surface equation. The partial differential equations are converted into ordinary ones by substituting the obtained velocity potential and wave functions and using the Galerkin method. The natural frequencies of liquid sloshing and the fluid–structure coupled system, as well as hydrodynamic forces and moments, are analyzed.

3.1. Nonlinear System Model

The surface tension of the liquid is disregarded, and the tank is assumed to be rigid. The liquid domain, the disturbed liquid surface, and the container are denoted by τ , S_f , and S_w , respectively. The OXY coordinate system represents an inertial frame of reference, and its axes are fixed. The moving coordinate system oxy is fixed in the tank; its axes translate with respect to the inertial frame OXY due to horizontal excitation, and the x -axis coincides with the undisturbed liquid surface S_0 , as shown in Figure 2.

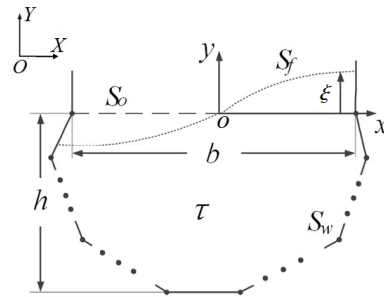


Figure 2. Coordinate systems.

The system’s kinetic energy is the sum of the kinetic energies of the tank and liquid, that is,

$$T = \frac{1}{2}M\dot{X}^2 + \frac{\rho}{2} \int_{\tau} (\nabla\Phi)^2 d\tau, \tag{6}$$

where M is the mass of the tank; X is the horizontal displacement of the tank; ρ is the liquid density; and Φ is the liquid velocity potential function under moving boundary conditions. Φ satisfies $\nabla^2\Phi = 0$ and $\frac{\partial\Phi}{\partial x} = \dot{X}$, so it can be expressed as $\Phi = \phi + x\dot{X}$, where ϕ is the liquid velocity potential function under static boundary conditions calculated with Equation (4) for a complicated-shape tank.

The tank movement is translated along the horizontal direction, and the liquid surface tension is disregarded. Consequently, the potential energy of the system contains only the gravitational potential energy of the liquid, that is,

$$\Pi = \frac{1}{2}\rho g \int_{S_f} \zeta^2 dS, \tag{7}$$

where g is the acceleration of gravity.

The Hamilton–Ostrogradskiy principle indicates that

$$\int_{t_0}^{t_1} \left(\delta T - \delta \Pi + F\delta X + \int_{\tau} p \operatorname{div} \delta r d\tau \right) dt = 0, \tag{8}$$

where F is the force exerted on the rigid tank along the X -axis direction; p is the internal pressure of the liquid; and r denotes the relative position vector of liquid particles observed from the oxy coordinate system. The nonlinear fluid–structure coupled dynamic equations can then be obtained as (see Appendix A for details)

$$\begin{aligned} M\ddot{X} + \frac{d}{dt} \left(\rho \int_{\tau} \nabla\Phi d\tau \right) - F &= 0 \\ \frac{\partial\Phi}{\partial t} + \frac{1}{2}(\nabla\phi \cdot \nabla\phi) + g\zeta &= 0. \end{aligned} \tag{9}$$

The free surface of the liquid can be expressed as $F_f = \zeta(x, t) - y = 0$. Then, one has

$$\frac{\tilde{d}F_f}{dt} = \frac{\partial F_f}{\partial t} + \frac{\partial F_f}{\partial x} \frac{\partial x}{\partial t} + \frac{\partial F_f}{\partial y} \frac{\partial y}{\partial t} = 0. \tag{10}$$

Due to

$$\frac{\partial F_f}{\partial t} = \frac{\partial \zeta}{\partial t'} \frac{\partial x}{\partial t} = \frac{\partial \phi}{\partial x'} \frac{\partial y}{\partial t} = \frac{\partial \phi}{\partial y'} \tag{11}$$

the nonlinear kinetic sloshing equation can be obtained as

$$\frac{\partial \zeta}{\partial t} = -\nabla \phi \cdot \nabla F_f. \tag{12}$$

$u = [u_X, 0]$ is defined as the velocity of the tank, and $u_X = \dot{X}$. In the following part, the wave height ζ and velocity potential function ϕ in Equations (4) and (5) are truncated at the third order. ζ and ϕ are substituted into Equations (9) and (12), and the Galerkin method is used. Coupling ordinary differential equations with square and cubic nonlinear terms can be obtained as follows:

$$\begin{aligned} \dot{u}_X + \sum_{i=1}^3 \dot{u}_i \left(\lambda_i + \sum_{j=1}^3 \kappa_{ij} v_j + \sum_{j=0}^2 \sum_{k=0}^{2-j} \gamma_{ijkl} |_{(l=2-j-k)} v_1^j v_2^k v_3^{2-j-k} \right) \\ + \sum_{i=1}^3 \sum_{j=1}^3 \dot{v}_i u_j \left(\sigma_{ij} + \sum_{k=1}^3 \omega_{ijk} v_k \right) + \gamma_x F_x = 0, \\ \sum_{j=1}^3 a_{ij} \dot{u}_j + a_{iX} \dot{u}_X + \sum_{j=0}^2 \sum_{k=0}^{2-j} b_{ijkl} |_{(l=2-j-k)} u_1^j u_2^k u_3^{2-j-k} + \sum_{j=1}^3 v_j \left(c_{ij} + \right. \\ \left. \sum_{k=1}^3 d_{ijk} \dot{u}_k + \sum_{k=0}^2 \sum_{r=0}^{2-k} e_{ijkrl} |_{(l=2-k-r)} u_1^k u_2^r u_3^{2-k-r} \right) = 0, i = 1, 2, 3, \\ \sum_{j=1}^3 f_{ij} \dot{v}_j + \sum_{j=1}^3 u_j \left(-f_{ij} + \sum_{k=1}^3 h_{ijk} v_k + \right. \\ \left. \sum_{k=0}^2 \sum_{r=0}^{2-k} m_{ijkrl} |_{(l=2-k-r)} v_1^k v_2^r v_3^{2-k-r} \right) = 0, i = 1, 2, 3, \end{aligned} \tag{13}$$

where $\lambda_i, \kappa_{ij}, \gamma_{ijkl}, \sigma_{ij}, \omega_{ijk}, \gamma_x, a_{ij}, a_{iX}, b_{ijkl}, c_{ij}, d_{ijk}, e_{ijkrl}, f_{ij}, h_{ij},$ and m_{ijkrl} are constants.

3.2. Natural Frequencies

If the tank movement along the horizontal direction matches a given time-varying pattern, then the control force exerted on the tank can be calculated by the first equation, and the natural frequencies of liquid sloshing can be obtained by the second and third equations of (13). If the control force matches a given time-varying pattern, then the natural frequencies of the fluid–structure coupled system can be computed by all three equations of (13).

3.2.1. Natural Frequencies of Liquid Sloshing

In this case, the tank movement along the horizontal direction varies only with time and is unaffected by liquid sloshing; moreover, the time variation is given. Thus, in light of liquid sloshing, \dot{u}_X can be considered the excitation related to time. Mass matrix M and stiffness matrix K are

$$M = \begin{pmatrix} a_{11} & a_{12} & a_{13} \\ a_{21} & a_{22} & a_{23} \\ a_{31} & a_{32} & a_{33} \end{pmatrix}, \quad K = \begin{pmatrix} c_{11} & c_{12} & c_{13} \\ c_{21} & c_{22} & c_{23} \\ c_{31} & c_{32} & c_{33} \end{pmatrix}. \tag{14}$$

The eigenvalue equation can then be written as

$$|K - M\omega^2| = 0. \tag{15}$$

The positive roots of ω^2 for Equation (15) are the first three orders of natural frequencies of liquid sloshing in complicated-shape tanks.

3.2.2. Natural Frequencies of the Fluid–Structure Coupled System

In this case, the variation in control force F_x with time during the entire movement is given, where F_x is exerted on the tank along the horizontal direction. Therefore, the tank movement is related to liquid sloshing; i.e., the motions of the liquid and the tank are coupled. Mass matrix \tilde{M} and stiffness matrix \tilde{K} are

$$\tilde{M} = \begin{pmatrix} a_{11} - a_{1X}\lambda_1 & a_{12} - a_{1X}\lambda_2 & a_{13} - a_{1X}\lambda_3 \\ a_{21} - a_{2X}\lambda_1 & a_{22} - a_{2X}\lambda_2 & a_{23} - a_{2X}\lambda_3 \\ a_{31} - a_{3X}\lambda_1 & a_{32} - a_{3X}\lambda_2 & a_{33} - a_{3X}\lambda_3 \end{pmatrix},$$

$$\tilde{K} = \begin{pmatrix} c_{11} & c_{12} & c_{13} \\ c_{21} & c_{22} & c_{23} \\ c_{31} & c_{32} & c_{33} \end{pmatrix}. \quad (16)$$

The eigenvalue equation can then be written as

$$|\tilde{K} - \tilde{M}\omega^2| = 0. \quad (17)$$

The positive roots of ω^2 for Equation (17) are the first three orders of natural frequencies of the fluid–structure coupled system in complicated-shape tanks.

3.3. Slosh Forces and Moments

The forces and moments of liquid sloshing on the tank are the results of the integral of the pressure on the boundary. The pressure p of the liquid in the tank can be expressed in terms of velocity potential by using the Cauchy–Lagrange integral equation,

$$p = -\rho \left[g\xi + \frac{\partial\Phi}{\partial t} + \frac{1}{2}(\nabla\phi)^2 + c(t) \right], \quad (18)$$

where $c(t)$ is an arbitrary time-dependent function. Considering that the surface tension of the liquid is disregarded, one has $c(t) = -\frac{p_0(t)}{\rho}$, where $p_0(t)$ is the pressure gas above the liquid surface; $p_0(t)$ can be omitted, i.e., $c(t) = 0$, because the entire system is submerged in the air with gas pressure, which is the same at each point.

The z -axis is defined along the normal direction of the x - y plane and completes the right-handed system. A 2D sloshing problem is considered in this study, and F_x and M_z are involved.

$$F_x = \int_{S_w} p \cos(\mathbf{n}, x) dS,$$

$$M_z = \int_{S_w} p [x \cos(\mathbf{n}, y) - y \cos(\mathbf{n}, x)] dS, \quad (19)$$

where \mathbf{n} is the unit vector along the normal direction at the point on S_w . The slosh moment is about the origin o of the moving coordinate system oxy fixed on the tank.

4. Discussion

The liquid sloshing problem in the Cassini-section-shape tank is analyzed with the proposed semi-analytical method, in which a fourth-order polynomial is adopted to fit the approximate analytical function. With regard to the case wherein the tank movement is given, the analysis results of natural frequencies, slosh forces, and moments are compared with the results of numerical simulations.

4.1. Approximate Mapping Function

Figure 3 shows the Cassini section shape with walls that are vertical and a bottom that is a semicircle, which is the liquid-filled and nearby areas of the full, closed container. As an example, we suppose that the width of the liquid surface is $b = 4$ m, the radius of

the semicircle is $R = \frac{b}{2}$, the depth of the liquid along the two walls is h , and h is set at 0, 0.5, 1, and 1.5 m for four different cases. The liquid density is $\rho = 1000 \text{ kg/m}^3$, and the mass of the tank is set at $M = 600 \text{ kg}$.

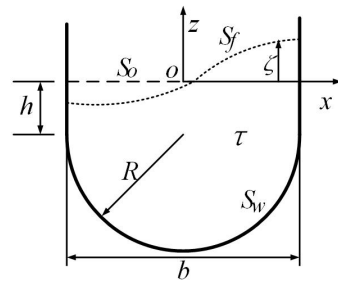


Figure 3. Cassini shape tank.

The curved boundary, i.e., the semicircle in this case, is contained in the Cassini shape, and a sixteen-sided polygon is used to substitute for the semicircle. The approximate expressions can be obtained based on Schwarz–Christoffel mapping and polynomial fitting, and the specified coefficients α_{ij} and β_{ij} in Equation (3) for different h are given in Tables A1 and A2 (Appendix B). The rest of the α_{ij} and β_{ij} values that are not listed in Tables A1 and A2 are all equal to zero.

4.2. Analysis and Comparison

The ordinary differential equations can be obtained for fluid–structure coupled dynamics with the Cassini-section-shaped tank by substituting the above fourth-order approximate analytical mapping functions into the velocity potential and wave height functions (4) and (5), substituting ϕ and ζ into the dynamic and kinetic Equations (9) and (12), and using the Galerkin method. The natural frequencies of liquid sloshing and the fluid–structure coupled systems can be calculated for different h by using Equations (15) and (16). Table 1 shows that the first-order and third-order natural frequencies for the fluid–structure coupled system are larger than those for liquid sloshing, especially for the first order, and the maximum difference is 30%; however, the second-order natural frequencies for these two cases are almost equal. Simultaneously, natural frequencies are analyzed with the numerical software DampSlosh, but only the ones for liquid sloshing can be analyzed. Therefore, comparisons of theoretical and numerical results are only conducted for the natural frequencies of liquid sloshing. The results agree well. The maximum relative error is about 5%, as shown in Figure 4.

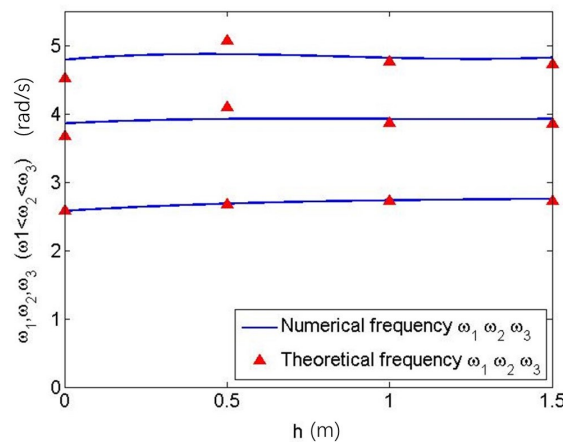


Figure 4. Comparisons of theoretical and numerical natural frequencies.

Table 1. Natural frequencies for different h .

h (m)	Frequencies for Liquid Sloshing (rad/s)			Frequencies for Coupled System (rad/s)		
	1st Order	2nd Order	3rd Order	1st Order	2nd Order	3rd Order
0	2.586	3.671	4.525	3.350	3.671	4.562
0.5	2.678	4.095	5.070	3.355	4.095	5.153
1	2.719	3.868	4.761	3.233	3.868	4.807
1.5	2.724	3.851	4.7291	3.184	3.851	4.762

The slosh forces and moments were obtained with Equations (18) and (19) and analyzed with the numerical software Flow3D. Only the case wherein the tank movement is given can be analyzed with Flow3D, so comparisons of theoretical and numerical results were only conducted for this case. The tank movement is given by $X = A \sin(\Omega t)$, where $A = 0.005$ m, and Ω is chosen as $\omega_i, i = 1, 2, 3$, which denotes the i -th order natural frequency. The slosh forces, slosh moments, and wave function coefficients for the first third-order modes with different wave heights, where $h = 0, 0.5, 1, 1.5$, are shown in Figures 5–8. By adopting the proposed semi-analytical method, regardless of which ω_i is selected as the excitation frequency, both sloshing forces and moments are in good agreement with the ones simulated with Flow3D for all cases with different h . A large wave height h leads to large sloshing forces and moments because the liquid mass increases with h . Sloshing forces and moments are the most violent when $\Omega = \omega_1$, followed by $\Omega = \omega_3$ and $\Omega = \omega_2$, as shown in Figures 5–8. All order modes of the liquid are activated simultaneously due to the nonlinear coupling terms in the dynamics, unlike the phenomenon in linear systems. In particular, for the case of $\Omega = \omega_2$, although it is excited at the second-order natural frequency, the amplitudes of coefficients $v_1(t)$ and $v_3(t)$ for the first-order and third-order modes are larger than the coefficient $v_2(t)$ for the second-order mode regardless of the value of h , as shown in Figures 5–8. Therefore, the second-order mode is a minor one and the odd-order modes are the major ones for liquid sloshing in the Cassini-section-shape tank. According to the comparison with the numerical results calculated with numerical software, the theoretical results obtained by the semi-analytical method are valid.

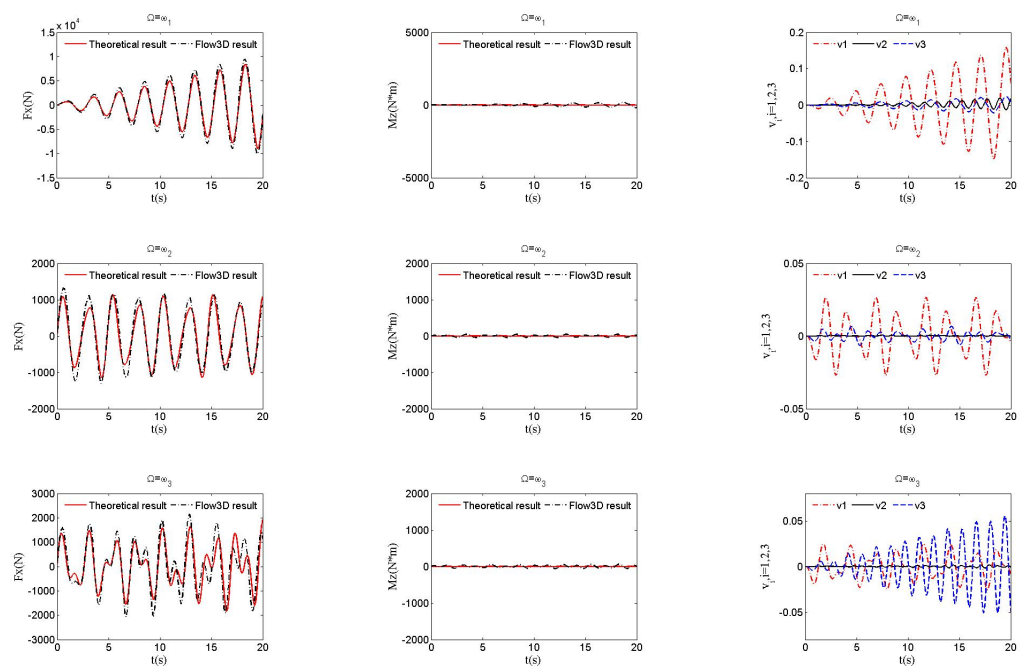


Figure 5. Slosh forces, moments, and coefficients of wave function at $h = 0$.

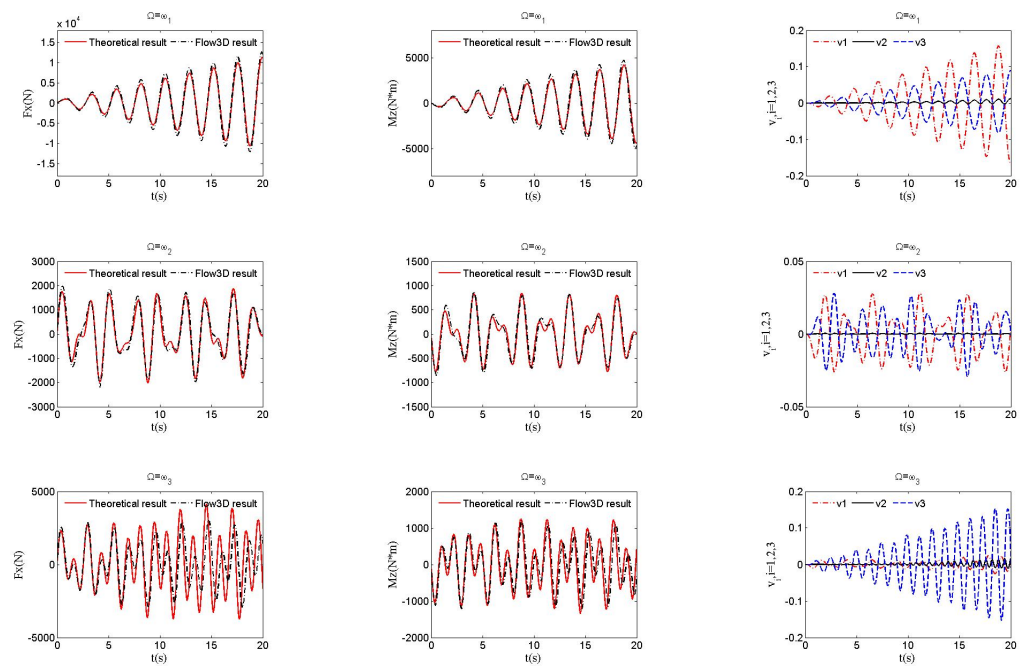


Figure 6. Slosh forces, moments, and coefficients of wave function at $h = 0.5$.

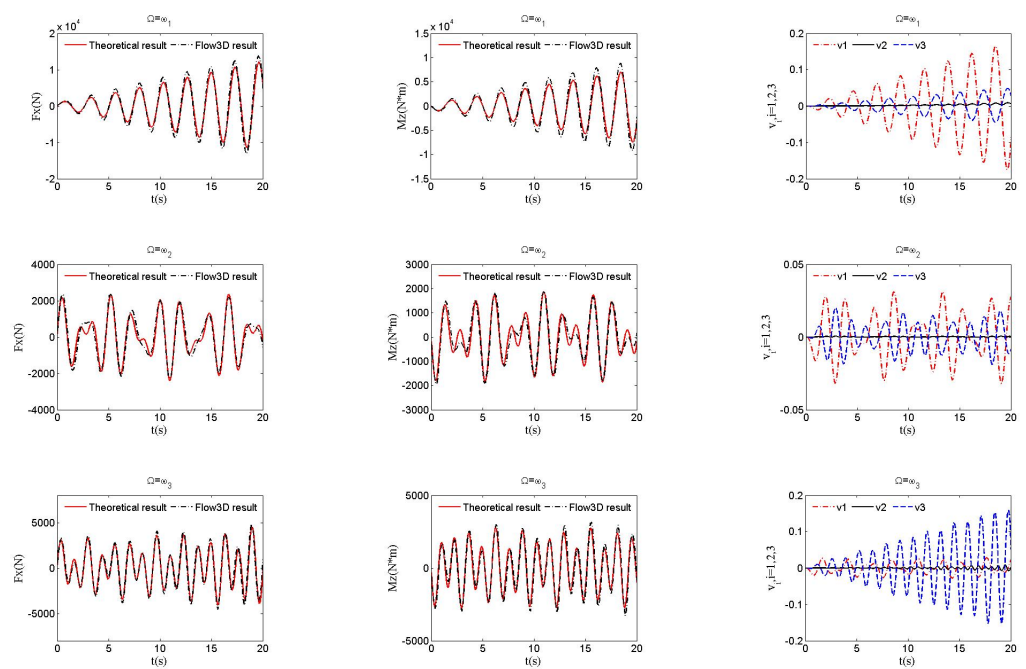


Figure 7. Slosh forces, moments, and coefficients of wave function at $h = 1$.

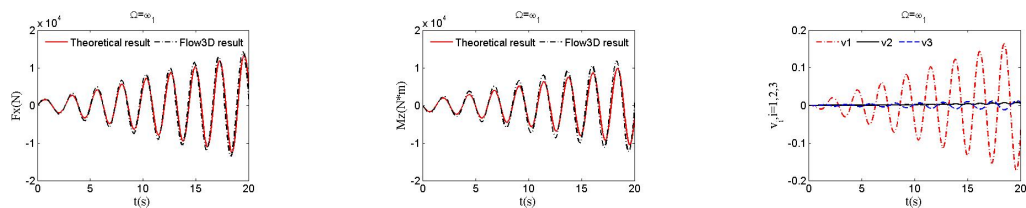


Figure 8. Cont.

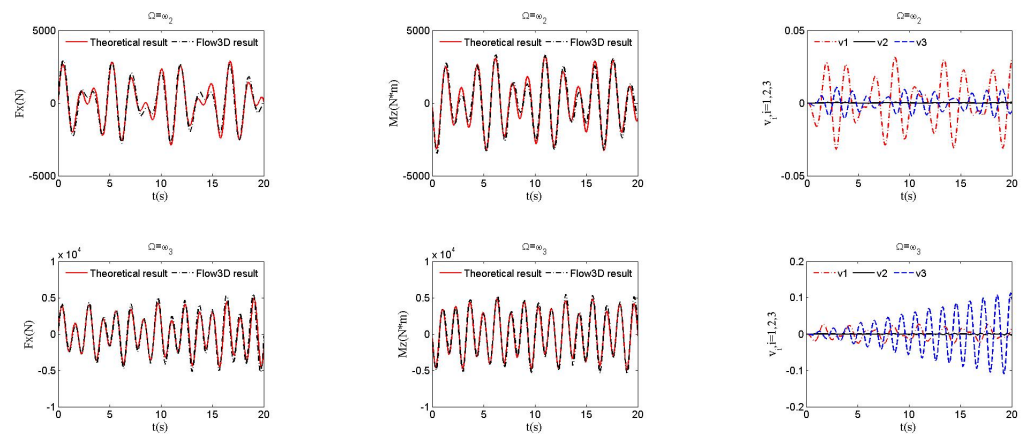


Figure 8. Slosh forces, moments, and coefficients of wave function at $h = 1.5$.

5. Conclusions

In this study, a semi-analytical method is proposed to solve the liquid sloshing problem in complicated-shape tanks with horizontal excitation. The difficulty of extending the conformal mapping method to solve the sloshing problem in highly complicated-shape tanks is determining the analytical mapping function between a complicated shape and a simple one. In this method, the approximate analytical mapping function between a complicated shape and a rectangle, which can be obtained by combining the Schwarz–Christoffel transformation and polynomial fitting, is used. The Schwarz–Christoffel transformation is utilized for point mapping, and the polynomial fitting method is adopted to obtain the final approximate analytical mapping function. Subsequently, dynamic and kinematic equations are derived based on the Hamilton–Ostrogradskiy principle and the relationship between the liquid velocity and the free-surface equation. Natural frequencies, hydrodynamic forces, and moments are analyzed.

The liquid sloshing problem in a Cassini-section-shape tank was studied with the proposed semi-analytical method. It was found that the first-order and third-order natural frequencies for the fluid–structure coupled system are larger than those for liquid sloshing, and the second-order natural frequencies for the two cases are almost equal. Sloshing forces and moments are the most violently excited at the first-order natural frequency, followed by the third-order frequency and second-order frequency. All order modes of the liquid are activated due to the nonlinear coupling dynamics. Furthermore, the second-order mode is a minor one and the odd-order modes are the major ones for liquid sloshing in the Cassini-section-shape tank. The semi-analytical results agree well with the numerical ones calculated with numerical software.

However, liquid sloshing analysis was studied only for 2D problems in this work. An interesting topic for further research is the extension of the results to 3D sloshing problems. Another topic worthy of investigation is the in-depth analysis of nonlinear dynamics.

Author Contributions: Conceptualization, J.L.; methodology, X.Z.; validation, J.L. and Y.Y.; formal analysis, X.Z. and Y.Y.; investigation, J.L. and Y.Y.; visualization, J.L. and X.Z.; writing—original draft preparation, J.L. and X.Z.; writing—review and editing, J.L., X.Z. and Y.Y.; supervision, Y.Y.; funding acquisition, J.L. All authors have read and agreed to the published version of the manuscript.

Funding: This research received no external funding.

Data Availability Statement: The original contributions presented in the study are included in the article, further inquiries can be directed to the corresponding authors.

Conflicts of Interest: The authors declare no conflicts of interest.

Appendix A

If the liquid is incompressible, then $\text{div} \delta \mathbf{r} = 0$. Given $p \text{div} \delta \mathbf{r} = \text{div}(p \delta \mathbf{r}) - \nabla p \cdot \delta \mathbf{r}$, based on Gauss's law, one has $\int_{\tau} \text{div}(p \delta \mathbf{r}) d\tau = \int_{S_f+S_w} p \delta \mathbf{r} \cdot d\mathbf{S}$. The normal relative velocity is zero at the wall and the bottom of the tank, i.e., $\mathbf{n} \cdot \delta \mathbf{r} = 0$ on S_w ; thus, $\int_{\tau} \text{div}(p \delta \mathbf{r}) d\tau = \int_{S_f} p \mathbf{n} \cdot \delta \mathbf{r} dS$, where \mathbf{n} is the unit vector along the normal direction at the point on S_w and S_f . $\frac{d}{dt}$ is defined as the time derivative observed from the space-fixed coordinate system OXY , and $\frac{\tilde{d}}{dt}$ is the time derivative observed from the tank-fixed coordinate system oxy . Given $\nabla \Phi = [\dot{X}, 0] + \dot{\mathbf{r}}$, one has

$$\begin{aligned} & \int_{t_0}^{t_1} \left(\delta T - \delta \Pi + F \delta X + \int_{\tau} p \text{div} \delta \mathbf{r} d\tau \right) dt \\ &= \int_{t_0}^{t_1} \left[M \ddot{X} \delta \dot{X} + \rho \int_{\tau} \nabla \Phi \cdot \delta(\nabla \Phi) d\tau - \rho g \int_{S_f} \xi \delta \xi dS \right. \\ & \quad \left. + F \delta X + \int_{S_f} p \mathbf{n} \cdot \delta \mathbf{r} dS - \int_{\tau} \nabla p \cdot \delta \mathbf{r} d\tau \right] dt \\ &= \int_{t_0}^{t_1} \left[M \dot{X} \delta \dot{X} + \rho \int_{\tau} \nabla \Phi d\tau \delta \dot{X} + \rho \int_{\tau} \nabla \Phi \cdot \delta \mathbf{r} d\tau \right. \\ & \quad \left. - \rho g \int_{S_f} \xi \delta \xi dS + F \delta X + \int_{S_f} p \mathbf{n} \cdot \delta \mathbf{r} dS - \int_{\tau} \nabla p \cdot \delta \mathbf{r} d\tau \right] dt \\ &= \int_{t_0}^{t_1} \left[\frac{d}{dt} (M \dot{X} \delta X) - M \ddot{X} \delta X + \frac{d}{dt} \left(\rho \int_{\tau} \nabla \Phi d\tau \delta X \right) - \frac{d}{dt} \left(\rho \int_{\tau} \nabla \Phi d\tau \right) \delta X \right. \\ & \quad \left. + \rho \int_{\tau} \frac{\tilde{d}}{dt} (\nabla \Phi \cdot \delta \mathbf{r}) d\tau - \rho \int_{\tau} \frac{\tilde{d}}{dt} (\nabla \Phi) \cdot \delta \mathbf{r} d\tau - \rho g \int_{S_f} \xi \delta \xi dS \right. \\ & \quad \left. + F \delta X + \int_{S_f} p \mathbf{n} \cdot \delta \mathbf{r} dS - \int_{\tau} \nabla p \cdot \delta \mathbf{r} d\tau \right] dt. \tag{A1} \end{aligned}$$

\dot{X} represents the tank movement, and it is irrelevant to x , y , and z . $\nabla(\nabla \phi) \cdot \nabla \phi = \frac{1}{2} \nabla(\nabla \phi \cdot \nabla \phi) - \nabla \phi \times (\nabla \times \nabla \phi)$, with $\nabla \times \nabla \phi = 0$ for irrotational liquid, so $\nabla(\nabla \phi) \cdot \nabla \phi = \frac{1}{2} \nabla(\nabla \phi \cdot \nabla \phi)$. Therefore,

$$\begin{aligned} \frac{\tilde{d}(\nabla \Phi)}{dt} &= \frac{\partial(\nabla \Phi)}{\partial x} \frac{\partial x}{\partial t} + \frac{\partial(\nabla \Phi)}{\partial y} \frac{\partial y}{\partial t} + \frac{\partial(\nabla \Phi)}{\partial z} \frac{\partial z}{\partial t} + \frac{\partial(\nabla \Phi)}{\partial t} \\ &= \frac{\partial(\nabla \phi)}{\partial x} \frac{\partial x}{\partial t} + \frac{\partial(\nabla \phi)}{\partial y} \frac{\partial y}{\partial t} + \frac{\partial(\nabla \phi)}{\partial z} \frac{\partial z}{\partial t} + \frac{\partial(\nabla \phi)}{\partial t} \\ &= \nabla(\nabla \phi) \cdot \nabla \phi + \frac{\partial(\nabla \phi)}{\partial t} \\ &= \frac{1}{2} \nabla(\nabla \phi \cdot \nabla \phi) + \frac{\partial(\nabla \phi)}{\partial t}. \tag{A2} \end{aligned}$$

Equation (A2) and $\mathbf{n} \cdot \delta \mathbf{r} = \delta \xi$ on S_f imply that Equation (A1) can be rewritten as

$$\begin{aligned} & \int_{t_0}^{t_1} \left(\delta T - \delta \Pi + F \delta X + \int_{\tau} p \text{div} \delta \mathbf{r} d\tau \right) dt \\ &= \int_{t_0}^{t_1} \left\{ \left[-M \ddot{X} - \frac{d}{dt} \left(\rho \int_{\tau} \nabla \Phi d\tau \right) + F \right] \delta X - \rho \int_{\tau} \nabla \left(\frac{\partial \Phi}{\partial t} \right. \right. \\ & \quad \left. \left. + \frac{1}{2} (\nabla \phi \cdot \nabla \phi) + p \right) \cdot \delta \mathbf{r} d\tau - \rho g \int_{S_f} \xi \delta \xi dS + \int_{S_f} p \delta \xi dS \right\} dt \\ & \quad + \left[\left(M \dot{X} + \rho \int_{\tau} \nabla \Phi d\tau \right) \delta X + \rho \int_{\tau} (\nabla \Phi \cdot \delta \mathbf{r}) d\tau \right] \Big|_{t_0}^{t_1}. \tag{A3} \end{aligned}$$

Similar to $p \operatorname{div} \delta \mathbf{r} = \operatorname{div}(p \delta \mathbf{r}) - \nabla p \cdot \delta \mathbf{r}$, and $\operatorname{div} \delta \mathbf{r} = 0$ for incompressible liquid, one has

$$\begin{aligned} & \nabla \left(\frac{\partial \Phi}{\partial t} + \frac{1}{2}(\nabla \phi \cdot \nabla \phi) + p \right) \cdot \delta \mathbf{r} \\ &= \operatorname{div} \left[\left(\frac{\partial \Phi}{\partial t} + \frac{1}{2}(\nabla \phi \cdot \nabla \phi) + p \right) \delta \mathbf{r} \right] - \left(\frac{\partial \Phi}{\partial t} + \frac{1}{2}(\nabla \phi \cdot \nabla \phi) + p \right) \operatorname{div} \delta \mathbf{r} \\ &= \operatorname{div} \left[\left(\frac{\partial \Phi}{\partial t} + \frac{1}{2}(\nabla \phi \cdot \nabla \phi) + p \right) \delta \mathbf{r} \right]. \end{aligned} \tag{A4}$$

Based on Gauss’s law, $\mathbf{n} \cdot \delta \mathbf{r} = 0$ on S_w and $\mathbf{n} \cdot \delta \mathbf{r} = \delta \xi$ on S_f , one has

$$\begin{aligned} & \rho \int_{\tau} \nabla \left(\frac{\partial \Phi}{\partial t} + \frac{1}{2}(\nabla \phi \cdot \nabla \phi) + p \right) \cdot \delta \mathbf{r} d\tau \\ &= \rho \int_{S_f + S_w} \left(\frac{\partial \Phi}{\partial t} + \frac{1}{2}(\nabla \phi \cdot \nabla \phi) + p \right) \mathbf{n} \cdot \delta \mathbf{r} dS \\ &= \rho \int_{S_f} \left(\frac{\partial \Phi}{\partial t} + \frac{1}{2}(\nabla \phi \cdot \nabla \phi) + p \right) \delta \xi dS. \end{aligned} \tag{A5}$$

Furthermore, the integral conditions are $\delta X = 0$ and $\delta \mathbf{r} = \mathbf{0}$ at $t = t_0$ and $t = t_1$, so Equation (A3) can be rewritten as

$$\begin{aligned} & \int_{t_0}^{t_1} \left(\delta T - \delta \Pi + F \delta X + \int_{\tau} p \operatorname{div} \delta \mathbf{r} d\tau \right) dt \\ &= \int_{t_0}^{t_1} \left\{ \left[-M \ddot{X} - \frac{d}{dt} \left(\rho \int_{\tau} \nabla \Phi d\tau \right) + F \right] \delta X \right. \\ & \quad \left. - \rho \int_{S_f} \left(\frac{\partial \Phi}{\partial t} + \frac{1}{2}(\nabla \phi \cdot \nabla \phi) + g \xi \right) \delta \xi dS \right\} dt. \end{aligned} \tag{A6}$$

δX and $\delta \xi$ are independent, and the nonlinear fluid–structure coupled dynamic formulas in Equation (9) can then be obtained.

Appendix B

Table A1. The coefficients α_{ij} for different h .

h	α_{10}	α_{21}	α_{30}	α_{32}	α_{41}	α_{43}
0	1.012	0.136	−0.011	0.020	−0.090	0.063
0.5	0.814	−0.263	0.045	−0.429	−0.003	−0.101
1	0.903	−0.135	0.019	−0.194	−0.018	−0.025
1.5	0.957	−0.033	0.006	−0.052	−0.019	0.007

Table A2. The coefficients β_{ij} for different h .

h	β_{00}	β_{11}	β_{20}	β_{22}	β_{31}	β_{33}	β_{40}	β_{42}	β_{44}
0	−0.053	0.955	−0.009	−0.990	−0.012	−0.846	0.007	−0.173	−0.198
0.5	−0.010	0.539	0.082	−0.839	0.279	−0.566	−0.011	0.067	−0.109
1	−0.088	0.810	0.064	−0.516	0.121	−0.294	−0.009	−0.007	−0.044
1.5	−0.061	0.941	0.046	−0.230	0.035	−0.109	−0.009	−0.025	−0.011

References

1. Abramson, H.N. *The Dynamic Behavior of Liquids in Moving Containers*; NASA SP 106; NASA: Washington, DC, USA, 1966.
2. Ibrahim, R.A. *Liquid Sloshing Dynamics: Theory and Applications*; Cambridge University Press: Cambridge, UK, 2005.
3. Seyyed, M.H. Liquid Sloshing in half-full horizontal elliptical tanks. *J. Sound Vib.* **2009**, *324*, 332–349.
4. Ken, H. Lessons from the 2003 Tokachi-oki, Japan, earthquake for prediction of long-period strong ground motions and sloshing damage to oil storage tanks. *J. Seismol.* **2008**, *12*, 255–263.
5. Volkan, O.; Emanuele, B.; Roberto, N. Earthquake-induced nonlinear sloshing response of above-ground steel tanks with damped or undamped floating roof. *Soil Dyn. Earthq. Eng.* **2021**, *144*, 106673.
6. Faltinsen, O.M.; Rognebakke, O.F.; Lukovsky, I.A.; Timokha, A.N. Multidimensional modal analysis of nonlinear sloshing in a rectangular tank with finite water depth. *J. Fluid Mech.* **2000**, *407*, 201–234. [[CrossRef](#)]
7. Faltinsen, O.M.; Rognebakke, O.F.; Timokha, A.N. Resonant three-dimensional nonlinear sloshing in a square-base basin analysis of nonlinear sloshing in a rectangular tank. *J. Fluid Mech.* **2003**, *487*, 1–42. [[CrossRef](#)]
8. Takashi, I. Autoparametric resonances in elastic structures carrying two rectangular tanks partially filled with liquid. *J. Sound Vib.* **2007**, *302*, 657–682.
9. Takashi, I.; Yuji, H.; Takefumi, O. Internal resonance of nonlinear sloshing in rectangular liquid tanks subjected to obliquely horizontal excitation. *J. Sound Vib.* **2016**, *361*, 210–225.
10. Miles, J.W. Internally resonant surface waves in a circular cylinder. *J. Fluid Mech.* **1984**, *149*, 1–14. [[CrossRef](#)]
11. McIver, P. Sloshing frequencies for cylindrical and spherical containers filled to an arbitrary depth. *J. Fluid Mech.* **1989**, *201*, 243–257. [[CrossRef](#)]
12. Utsumi, M.A. Mechanical Model for Low-Gravity Sloshing in an Axisymmetric Tank. *J. Appl. Mech.* **2004**, *71*, 724–730. [[CrossRef](#)]
13. Yue, B.Z. Coupling Frequency of the Liquid Sloshing in a Cylindrical Tank with a Flexible Baffle. *J. Beijing Inst. Technol.* **2006**, *15*, 1–4.
14. He, Y.J.; Ma, X.R.; Wang, P.P.; Wang, B.L. Low-gravity liquid nonlinear sloshing analysis in a tank under pitching excitation. *J. Sound Vib.* **2007**, *299*, 164–177.
15. Hiroki, T.; Koji, K. Frequency response of sloshing in an annular cylindrical tank subjected to pitching excitation. *J. Sound Vib.* **2012**, *331*, 3199–3212.
16. Budiansky, B. Sloshing of liquids in circular canals and spherical tanks. *J. Aero/Space Sci.* **1960**, *27*, 161–172. [[CrossRef](#)]
17. Chu, W.H. Liquid sloshing in a spherical tank filled to an arbitrary depth. *AIAA J.* **1964**, *2*, 1972–1979. [[CrossRef](#)]
18. Fox, D.W.; Kuttler, J.R. Sloshing frequencies. *J. Appl. Math. Phys.* **1983**, *34*, 668–696. [[CrossRef](#)]
19. Seyyed, M.H.; Mostafa, A. Transient sloshing in half-full horizontal elliptical tanks under lateral excitation. *J. Sound Vib.* **2011**, *330*, 3507–3525.
20. Faltisen, O.M.; Timokha, A.N. A multimodal method for liquid sloshing in a two-dimensional circular tank. *J. Fluid Mech.* **2010**, *665*, 457–479. [[CrossRef](#)]
21. Faltisen, O.M.; Timokha, A.N. Multimodal analysis of weakly nonlinear sloshing in a spherical tank. *J. Fluid Mech.* **2013**, *665*, 457–479.
22. Bauer, H.F. Sloshing in conical tanks. *Acta Mech.* **1982**, *43*, 185–200. [[CrossRef](#)]
23. Gavriluk, I.; Lukovsky, I.A.; Timokha, A.N. Nonlinear sloshing in a circular conical tank. *Hybrid Methods Eng.* **2001**, *3*, 1–39. [[CrossRef](#)]
24. Lukovskii, I.A.; Timokha, A.N. Modal modeling of nonlinear fluid sloshing in tanks with non-vertical walls: Non-conformal mapping technique. *Int. J. Fluid Mech. Res.* **2002**, *29*, 216–242.
25. Chen, S.; Johnson, D.B.; Paad, P.E. Velocity boundary conditions for the simulation of free surface fluid flow. *J. Comput. Phys.* **1995**, *116*, 262–276. [[CrossRef](#)]
26. Yang, H.; West, J. Validation of high-resolution CFD method for slosh damping extraction of baffled tanks. In Proceedings of the 52nd AIAA/SAE/ASEE Joint Propulsion Conference, Salt Lake City, UT, USA, 25–27 July 2016; AIAA Paper 2016-4587.
27. Bass, R.L.; Bowels, E.B.; Endo, S.; Pots, B. Modeling criteria for scaled LNG sloshing experiments. *J. Fluids Eng.* **1985**, *107*, 272–280. [[CrossRef](#)]
28. Hung, R.J.; Long, Y.T. *Dynamical Models for Sloshing Dynamics of Helium II under Low-G Conditions*; NASA-CR-203845; NASA: Washington, DC, USA, 1997.
29. Takashi, N. ALE finite element computations of fluid-structure interaction problems. *Comput. Methods Appl. Mech. Eng.* **1994**, *112*, 291–308. [[CrossRef](#)]
30. Liu, M.B.; Liu, G.R. Smoothed Particle Hydrodynamics (SPH): An overview and recent developments. *Arch. Comput. Methods Eng.* **2010**, *17*, 25–76. [[CrossRef](#)]
31. Yu, Q.; Wang, T.; Li, Z. Rapid simulation of 3D liquid sloshing in the lunar soft-landing spacecraft. *AIAA J.* **2019**, *57*, 4504–4513. [[CrossRef](#)]
32. Vanyo, J.P. *Rotating Fluids in Engineering and Science*; Butterworth-Heinemann: Boston, MA, USA, 1993.
33. Nichkawde, C.; Harish, P.M.; Ananthkrishnan, N. Stability analysis of a multibody system model for coupled slosh-vehicle dynamics. *J. Sound Vib.* **2004**, *275*, 1069–1083. [[CrossRef](#)]
34. Gou, X.Y.; Li, T.S.; Ma, X.R.; Wang, B.L. Forces and moments of the liquid finite amplitude sloshing in a liquid-solid coupled system. *Appl. Math. Mech.* **2001**, *22*, 528–540. [[CrossRef](#)]

35. Lü, J.; Li, J.F.; Wang, T.S. Dynamic Response of a liquid-filled rectangular tank with elastic appendages under pitching excitation. *Appl. Math. Mech.* **2007**, *28*, 351–359. [[CrossRef](#)]
36. Yue, B.Z. Nonlinear coupled dynamics of liquid-filled spherical container in microgravity. *Appl. Math. Mech.* **2008**, *29*, 1085–1092. [[CrossRef](#)]
37. Saff, E.B.; Snider, A.D. *Fundamentals of Complex Analysis with Applications to Engineering and Science*; Prentice Hall: Hoboken, NJ, USA, 2007.

Disclaimer/Publisher’s Note: The statements, opinions and data contained in all publications are solely those of the individual author(s) and contributor(s) and not of MDPI and/or the editor(s). MDPI and/or the editor(s) disclaim responsibility for any injury to people or property resulting from any ideas, methods, instructions or products referred to in the content.